

Kerry Anderson¹
Canadian Forest Service

Al Pankratz, Curtis Mooney
Environment Canada

Kelly Fleetham
Alberta Environment and Sustainable Resource Development

1. INTRODUCTION

Predicting the possible penetration (injection) heights of smoke plumes from wildland forest fires is largely an unresolved problem (Heilman *et al.* 2014, Goodrick *et al.* 2013, Larkin *et al.* 2012). Until now, many approaches have followed those of air pollution plumes generated from tall chimneys. The relationship between the two is weak, as kinetic energy is a primary factor in chimney plumes while wildland fires are buoyancy driven.

In 2011, Anderson *et al.* provided a thermodynamic solution for predicting the penetration height of smoke plumes. Using the energy of the fire as input, it predicts the height of a column of air mixed from the environmental lapse rate to a dry adiabatic lapse rate, with the top of the column captured by the height of thermal equilibrium.

2. THEORY

A detailed description and solution for the thermodynamic plume rise model can be found in Anderson *et al.* 2011. The theory is briefly summarized as follows.

2.1 Plume Rise Model

The solution for the penetration height considers two principal factors: the energy being released into the atmosphere by the fire, and the ambient (environmental) lapse rate. More specifically, heat energy is mixed through a column of air above the fire until the column reaches thermal balance,

which is represented by the dry adiabatic lapse rate.

A thermodynamic solution to the penetration height of the smoke plume follows the approach illustrated in Figure 1. Heat produced from the fire is equated to the energy term, Q [J], which then modifies the column of air above the fire. The mass of the air column, M [kg], is required to solve the problem

2.2 Energy per Unit Mass

The energy per unit mass, $Q/M = q$, required to modify the atmosphere can be calculated using the tephigram (Fig. 1). The quantity q can be derived from an enclosed area on the tephigram as follows:

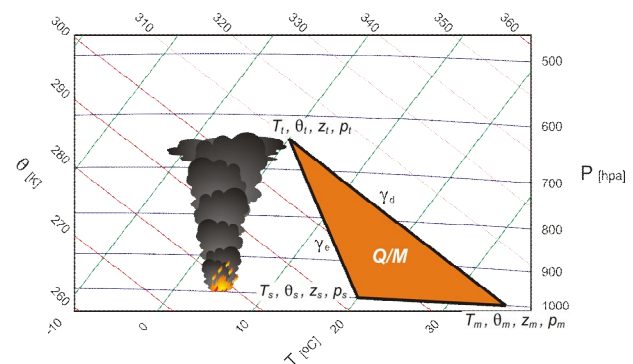


Figure 1. Representation of a smoke plume on a tephigram. Q is the energy of the fire that enters the plume while M is the mass of the plume. The orange triangle indicates the energy per mass Q/M , which is constrained by the environmental lapse rate γ_e , the dry adiabatic γ_d , and the surface pressure p_s . Values for the temperature, potential temperature, height and

¹ Corresponding author address: Kerry Anderson, Canadian Forest Service, Northern Forestry Centre, 5230 122 Street, Edmonton, AB, Canada, T6H 3S5; e-mail kanderso@nrcan.gc.ca

pressure (T , θ , z and p) can be determined at the surface, at the top and within the modified zone (subscripts s , t , and m).

$$(1) \quad q = -c_p \int T d \ln \theta$$

where q is the energy per unit mass [J kg^{-1}] released by the fire into the plume, c_p is the heat capacity of dry air [$1005 \text{ J kg}^{-1} \text{ K}^{-1}$], T is the temperature [K] and θ is the potential temperature [K].

Anderson *et al.* (2011) showed that

$$(2) \quad q = -\frac{1}{2} c_p \gamma_d \Delta z \ln \left[1 + \frac{\Delta z (\gamma_e - \gamma_d)}{T_s} \right]$$

where γ_e is the environmental lapse rate [K m^{-1}], γ_d the dry adiabatic lapse rate [$9.8 \times 10^{-3} \text{ K m}^{-1}$], Δz the plume height [m], and T_s the surface temperature [K]; and making use of

$$(3) \quad M = \frac{p_s}{g} A \left[1 - \left(1 + \frac{\gamma_e \Delta z}{T_s} \right)^{-g/\gamma_e R_d} \right]$$

where M is the mass of the plume [kg], p_s the surface pressure [pa], g the gravitational acceleration [-9.8 m s^{-2}], A the fire area [m^2] and R_d the gas constant [$287.05 \text{ J kg}^{-1} \text{ K}^{-1}$]. Together the solution for the thermodynamic plume rise then becomes

$$(4) \quad Q = q M$$

$$= -\frac{1}{2} p_s A \Delta z \ln \left[1 + \frac{\Delta z (\gamma_e - \gamma_d)}{T_s} \right] \times$$

$$\left[1 - \left(1 + \frac{\gamma_e \Delta z}{T_s} \right)^{-g/\gamma_e R_d} \right]$$

In its current form, Δz cannot be isolated to provide a solution for the plume height. Instead, an

iterative numerical procedure is used to converge on the answer. An estimate of the plume height, Δz is entered into the equation and the resulting value of Q is compared to the value of Q_{plume} from the fire. The plume height is then adjusted and the calculations are redone.

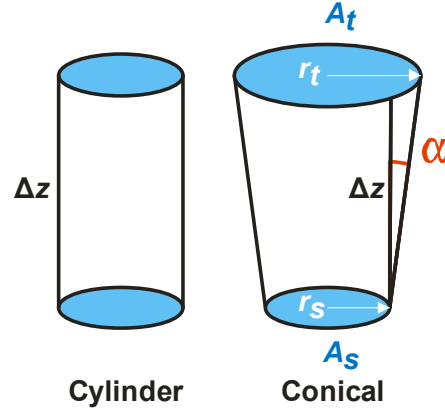


Figure 2. Possible plume shapes. The cylinder represents no entrainment as captured by equation 6 (with $\alpha=0$) The conical shape (with $\alpha>0$) assumes increasing plume width with height due to entrainment.

2.3 Entrainment

Entrainment can be captured within the model by modifying the plume shape (Fig. 2). One such modification is the conical shape, which increases the plume width with height. For a circular fire,

$$(5) \quad r_s = \sqrt{A_s / \pi}$$

$$(6) \quad r_t = r_s + \Delta z_e \tan \alpha$$

where r_s and r_t are the radii of the column at the surface and at the top, Δz_e is the adjusted entrainment height and α is the angle capturing the volume increase with height and thus the entrainment (typically 6-15°).

Keeping the mass of the affected volume constant (as calculated in equation 3), an average density $\bar{\rho}$ is calculated for the cylindrical column. This average density is used to calculate the mass of the expanding conical column as

$$(7) \quad M = \frac{1}{3} \pi \rho \Delta z_e (r_s^2 + r_s r_t + r_t^2)$$

and this term along with q from equation 2 is used in the convergence scheme (equation 4).

3. VALIDATION

A project is underway to measure the height of smoke plumes from wildland fires in Alberta. This study uses hand-held inclinometer measurements and photos taken at a number of lookout towers in the province. Equilibrium and maximum plume heights were measured based on the plume's final leveling height and the maximum lofting height respectively. Study results are presented, which are compared with the predicted heights based on the thermodynamic approach.

3.1 Methodology

This study currently includes four years of observations from 2010 to 2013, involving 13 fire observation lookout towers (Table 1).

Table 1. Lookout towers used in Alberta smoke plume observation study

Name	Latitude	Longitude	Platform Elevation (m ASL)
Keg	57.64	-118.35	980
Trout Mountain	56.80	-114.42	826
Whitefish	56.18	-115.47	735
Teepee Lake	56.46	-114.12	782
Kirby Lake	55.36	-110.65	691
Rainbow Lake	58.35	-119.71	601
Wadlin	57.78	-115.46	848
Livock	56.46	-113.02	650
Hotchkiss	57.33	-118.96	990
Hawk Hills	57.66	-117.42	730
Pinto	54.78	-119.40	1044
Battle River	57.17	-117.66	674
Saddle Hills	55.62	-119.72	967

During these years, 85 observations were collected. Five of these were rejected because

they were not reported wildland fires (plume IDs 29, 30, 50, 58, 63); three more were rejected because they did not report a mean plume height (only a maximum); and an additional seven were rejected due to modelling errors (as discussed in the results section). Of the remaining observations, there were 15 cases of fires being observed multiple times over the course of the day. For example, fire LWF090, May 24, 2013, was observed nine times from 8:35 to 17:05 MDT. In two cases, fire SWF120 (June 22, 2010) and fire PWF068 (July 11, 2012) were observed independently by two towers.



Figure 3. Illustration of the plume height observation and measurement.

Figure 3 illustrates the technique used to measure the smoke plume height based on the measured inclinometer angle. Taking the curvature of the Earth into account, the equation for the smoke plume height, Δz , is

$$(8) \quad \Delta z = D \tan \left[\tan^{-1} (D / 2R_e + z_T / D) + \theta \right]$$

where D is the distance from the tower to the fire, R_e is the radius of the Earth (6378.1 km), z_T is the height difference between the observing platform elevation and the fire base elevation, and θ is the angle from the horizontal to the top of the plume as measured by the inclinometer. The inclinometer used is a simple device, and while inexpensive and easy to use, there are issues related to its measurements. The device has a low resolution ($\pm 0.5^\circ$), and is prone to user reporting error. As noted later, in six cases the observations resulted in negative plume heights and were thus rejected.

It is also recognized that these Alberta plume observations are unverified against other data. There may be biases in the observations that could be reflected in the validation study. This is addressed in the discussion.

Fire behaviour conditions used in the study are

based on the Canadian Forest Fire Danger Rating System (CFFDRS). The surface, crown and total fuel consumptions (SFC, CFC, TFC) [kg m^{-2}] are based on the Canadian Fire Behaviour Prediction (FBP) System (Forestry Canada Fire Danger Working Group 1992). Alberta Provincial Forest Fire Centre fire assessment reports were used to guide the fire behaviour modelling decisions. In most cases, the C2 boreal spruce was noted as the FBP fuel type in the fire report. Canadian Forest Fire Weather Index (FWI) System inputs were interpolated from observations stored in the Canadian Wildland Fire Information System (CWFIS) (Van Wagner 1987; Englefield *et al.* 2001; Lee *et al.* 2002).

Values for the area burned at the time of plume observations (A_s) were derived from fire sizes at a time of assessment (not the same as the plume observation time) as provided by the provincial reports. In one case (fire PWF068) the assessment was conducted on the evening of the day previous to the plume observations (plume IDs 51, 52, 53). As the assessment occurred at 20:52 MDT, it was assumed that no further growth would occur that evening and that the fire size could be used as a starting size for the next day at 6:00 MDT. For large, multi-day fires, fire size was based on fire mapping techniques using infrared satellite imagery from polar orbiting satellites equipped with the Moderate Resolution Imaging Spectroradiometer (MODIS) sensor (Anderson *et al.* 2009). Finally, fire size at plume observation time was obtained by modelling fire growth between the assessed time and the plume observation time using elliptical fire growth (Forestry Canada Fire Danger Working Group 1992). The equations were applied in reverse to derive a time of ignition (or 6:00 MDT for larger fires), then recalculated forward in time to the plume observation time. The area value A_s used in equation 5 was set to the area burned during the 15 minutes prior to the plume observation time.

Energy entering the plume (Q) was derived from the total energy of the fire, which is the product of the fuel consumption (TFC), area burned (A_s) and the heat of combustion (H [$1.8 \times 10^7 \text{ J kg}^{-1}$]). It is recognized that not all the energy from the fire enters the plume. A certain amount goes into heating the fuel and evaporating the moisture, while some is lost into the soil and some is emitted horizontally as radiation (Byram 1959). Conducting

an energy balance of a fire is beyond the scope of this study. Instead it was decided to inject a fixed amount of the total energy of the fire into the plume. Through adjustment of the correlation scores shown later, it was found that applying 7% of the total energy of the fire to the energy of the plume produced the best results.

Lapse rate data were interpolated from the Global Environmental Multiscale (GEM) model runs conducted at the Canadian Meteorological Centre (Côté *et al.* 1998). Vertical profiles were created by extracting archived data on the GEM's native vertical coordinates (eta and hybrid levels, which are terrain-following pressure coordinates) using a linear interpolation from the four grid corners to the desired location. The lowest GEM hybrid level is intended to represent the surface, but the lowest dynamic level (the lowest layer to which the equations of motion are applied) is the next lowest level (about 40m above the ground). The GEM model uses a surface parameterization scheme based on output from this level to produce the surface values. Generally these values are reasonable but occasional super-adiabatic lapse rates occur in the lowest levels (which can be expected on a sunny summer afternoon).

The environmental lapse rate (γ_e) based on GEM profiles was calculated between the surface and standard pressure levels (850, 700 and 500 hpa). This follows the standard levels used by traditional convective indices such as the Showalter and Lifted indices. Super-adiabatic lapse rates ($< -9.8^\circ\text{C km}^{-1}$) were rejected from the analysis as this is beyond the physical assumption of the model; otherwise, lapse rates were limited to (and set to) a minimum of $-9.0^\circ\text{C km}^{-1}$ to avoid spurious results (when the term $\gamma_e - \gamma_d$ approaches zero, the solution tends to infinite height).

The environmental lapse rate γ_e , area burned A_s , and energy entering the plume Q were entered into equation 4 and the predicted plume height using the thermodynamic approach, Δz , was derived iteratively.

Plume height predictions were assessed based on lapse rates from the surface to 850 hpa, 700 hpa and 500 hpa, and from 850 hpa to 700 hpa and 500 hpa. Plume heights were also calculated using the Briggs model (1965, 1972), currently being used in

many smoke plume models including BlueSky (Larkin *et al.* 2009, Anderson *et al.* 2004). The method for calculating the Briggs plume height followed that described in the Fire Emission Production Simulator (FEPS) User's Guide (Anderson *et al.* 2004). Also, for comparison, the mixing layer height was calculated following the method described by Holzworth (1967).

Regression analysis was conducted between predicted and observed plume heights. Three separate tests were conducted to remove any bias created by multiple observations of the same fire on the same day. The first test included all plume observations; the second used the average of the observed plume heights with the time corresponding to when the observed plume height most closely matched the average; and the final test selected the observations closest to 17:00 LST (18:00 MDT), the time of peak burning conditions.

3.2 Results

Table 2 shows the 77 smoke plume observations for the Alberta smoke plume study. The table includes information on the fire and the observing station. Adjusted equilibrium plume height shows the observed height of the smoke plume, accounting for the curvature of the Earth following equation 8. Of the 77 observed plumes, six were rejected because the resulting adjusted plume heights were negative (plume IDs 2, 59, 65, 74, 76, 83). Also, one fire was rejected because fire-growth could not recreate the size at time of observation (45). This was likely due to an erroneous reporting date or size. The final number of fires used in the study was 70.

Table 3 shows the lapse rates extracted from the GEM archived data (350 in total). In 65 of the cases, super-adiabatic lapse rates were modelled by GEM (54 of the 65 observations for the surface to 850 hpa, 9 from the surface to 700 hpa; 2 from 850 to 700 hpa) and were rejected from the analysis. Another 60 cases had modelled lapse rates less than $-9.0^{\circ}\text{C km}^{-1}$ (but not super-adiabatic), which were adjusted to $-9.0^{\circ}\text{C km}^{-1}$.

The predicted plume heights shown in Table 3 were based on the lapse rates and using 7% of the fire's total energy as the energy injected into plume rise. Predicted plume heights ranged from 488 to 11,672 m for those with unadjusted lapse rates. In cases where the lapse rate was adjusted to -9.0°C

km^{-1} , plume heights ranged from 768 to 14 435 m.

Table 4 summarizes the correlations for the predicted plume heights using various lapse rates for the three studies. These result are also shown in Figure 4. The first study included all plume observations and had r^2 values ranging from 0.550 to 0.755; the second, which used the average of the observed plume heights for the day, had r^2 values ranging from 0.459 to 0.669; the final study, which used observations closest to 17:00 LST, had r^2 values ranging from 0.627 to 0.812.

The highest r^2 values corresponded to predictions based on the surface to 850 hpa lapse rates, yet these had the fewest number of observations with two-thirds of the lapse rates being rejected as super-adiabatic. As a result these should be regarded as having less value. Excluding these cases, the r^2 values range from 0.550 to 0.775. Predictions based on observations closest to 17:00 LST were the best at predicting the plume height, while the poorest predictions were based on the daily average of the observations. This is consistent with the assumption that the CFFDRS is most representative of fire behavior at 17:00 LST.

The Briggs method for the three studies had r^2 of 0.504, 0.481, 0.731. While not substantially lower than those produced using the thermodynamic approach, they were lower than 12 of the 15 thermodynamic model predictions (Fig. 4). The best predictions were for those closest to 17:00 LST suggesting that this may be the best representative time for those predictions.

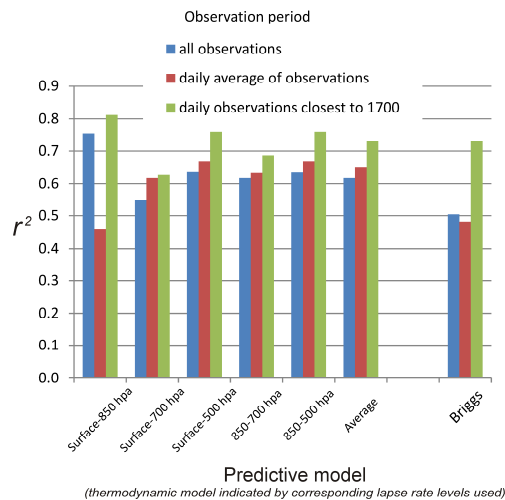


Figure 4. Histogram of correlation coefficients for the Alberta plume study by predictive model and by observation period. The average values are the average of the results less the surface to 850 hpa results.

Plume heights based on the mixing layer height produced a negligible correlation. This may be a function of the inherent smoothing associated with numerical modeling or a function of the 5°C offset applied to the surface temperature in Holtzworth’s method (Holtzworth, 1967). While a more rigorous approach could have improved results, it was deemed not worth pursuing.

Figure 5 shows a scatter plot of observed versus predicted plume heights using the Briggs model and using the heights predicted using the surface to 500 hpa lapse rate. This serves as an example of the predictability that is possible when using a single lapse rate. As is apparent from the plot, the Briggs model produced a dichotomous scatter with a large population of predictions near zero. The thermodynamic model produced a more even distribution of predictions though generally at a higher altitude than observed. An examination of the tabulated Briggs values indicates 36 out of the 77 predictions were under 100 m while three predictions were above 10,000 m (11,970, 12,541, and 14,451 m). The thermodynamic model predicted lower heights for the same plumes (9,064, 8,603 and 10,522 using the surface to 500 hpa lapse rate) but both models were much higher than the observed heights for these plumes (2,657, 4,760 and 8,828 m). Coincidentally, these plume observations and predictions are from the same fire (MWF007).

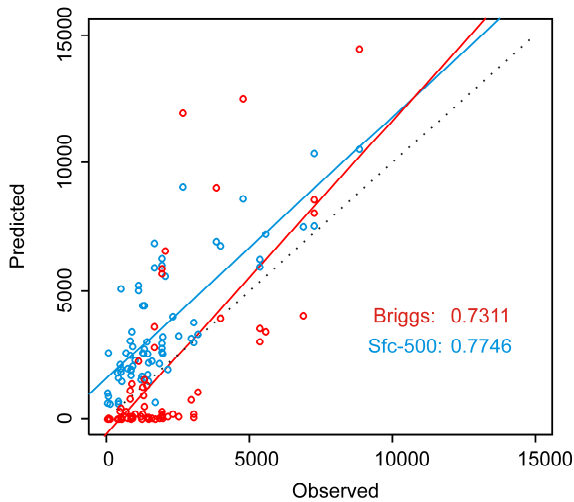


Figure 5. Scatter plot of predicted versus observed

plumes from the Alberta plume study. Thermodynamic model predictions based on the surface to 500 hpa lapse rate are shown in blue, Briggs model prediction shown in red. Predicted equals observed shown as black dashed line. Observed plume heights are limited to daily observations closest to 17:00 LST.

4. DISCUSSION

The thermodynamic solution presented in this paper is a model for the simple case of a column expanding vertically in an environment with a constant lapse rate and little wind. There is no exchange of energy between the column and the air outside the smoke column. It is assumed there is a combustion zone at the base of the column. A circulation is present where external air is brought in at the surface into the combustion zone and air exits at the top of the column. No energy is exchanged in these parts of the circulation. There is only a minor temporal component to this model captured by black body radiation, fire growth and the diurnal trend of the Fine Fuel Moisture Code (FFMC). The model predicts the plume height after thermal equilibrium within the column has been achieved, and does not capture buoyant development over time. In addition, the model does not take into account elevated inversions which could inhibit plume rise significantly.

Results from the Alberta smoke plume study show a clear correlation between the predicted and observed plume heights. With that said, problems with the observations (e.g. negative plume heights) and a lack of independent verification of the plume observations make the strength of the correlation difficult to assess.

There were two cases where two towers reported the same plume. On June 22, 2010, Trout Mountain and Teepee Lake both observed the plume from fire SWF120 (from 72 and 94 km respectively). Trout Mountain’s reported a maximum plume height (plume ID 5, not shown on Table 3) of 6,724 m at 16:30, while reports from Teepee Lake were 2,068 at 14:14 and 7,264 m at 17:53 (plume IDs 18, 19). Predictions among the various models were between 6,000 and 8,000. While Trout Mountain was reporting a maximum plume height, its observation fell within the plume development observed by Teepee Lake. Also, the observations by both towers fall within the range of model predictions,

On July 11, 2012 the plume from fire PWF068 was observed by both Hotchkiss and by Saddle Hills lookouts (from 23 and 173 km respectively). At 15:55 and again at 17:22 Hotchkiss reported a maximum height of 4,597 m while Saddle Hills reported a maximum height of 5,356 m at 16:12 and at 16:58. This report would suggest at least a +20% error in height measurements. Predictions from the models were approximately 8,000 m for the thermodynamic model and 3,000 m for the Briggs model.

The thermodynamic model shows a bias towards over-prediction in the lower range. A majority of the plumes observed below 2,000 m were predicted to rise to heights between 2,000 and 4,000 m. It is possible that the lower observed plume heights were because the plume tops were thin and poorly defined making them hard to observe. Alternatively, a strong inversion overlooked by the single lapse rate approach used by the thermodynamic model could be capping the plume at a lower height. Another possible source of over-prediction would be due to the choice of fuel types. The C2 Boreal Spruce fuel type displays the most intense fire behaviour characteristics of the FBP fuel types. While C2 is the predominant fuel type in northern Alberta, there may have been other fuel types involved. A closer examination of each fire would be useful in order to confirm the most representative fuel type and hence fire behaviour. Finally, it is assumed the fire area used in the model is a continuous zone filled with fuel and that all the fuel burns. Any irregularities or discontinuities in the fuels (open fields, streams, barren ground, etc.) are not accounted for in the area burned or the energy of the fire.

The energy entering the plume is dependent on the Surface Fuel Consumption (SFC), which, in turn, is dependent on the Build-up Index (BUI) of the Canadian Forest Fire Danger Rating System (Forestry Canada Fire Danger Group 1992). The BUI does not display a diurnal trend like the Fine Fuel Moisture Code (FFMC, Van Wagner 1987). As a result, the plume rise model may over-predict fire intensities and plume heights during periods outside of peak burning conditions.

In terms of observation data, the heights observed are in need of validation using an independent method. In addition, the thermodynamic method used in this paper breaks down when the environmental lapse rate is the same as the dry

adiabatic lapse rate through significant depths of the atmosphere.

An effort is now underway to use satellite-measured plume heights collected by MISR as was done by Sofiev *et al.* (2006) and Raffuse *et al.* (2012). This will require cross-referencing plumes with modelled profiles, provincial fire reports and fire weather conditions. Another effort is underway to refine this method by considering the entire profile in the calculation, not just the 850, 700 and 500 mb levels. In the interim, the thermodynamic model is being adapted for inclusion in the BlueSky framework as an optional plume rise model with possible links to an operational fire-growth model in the near future (Anderson *et al.* 2009).

5. CONCLUSIONS

A method was developed to predict smoke plume heights using a thermodynamic approach. This approach is based on fire size, energy released into a smoke plume and adiabatic lift to a level of thermal equilibrium with the environment.

A validation study was conducted using four years of field observations of smoke plumes from fire lookout towers. Results indicate a correlation between predicted and observed plume heights with r^2 values ranging from 0.459 to 0.812. The accuracy of the observations may be an issue and thus the performance of the thermodynamic approach presented may vary from the results shown.

Predicted plume heights utilizing the thermodynamic approach were compared to those predicted by the Briggs model, and to the mixing layer height. The latter produced no correlation. The Briggs model produced weaker but comparable correlations with the r^2 values range from 0.481 to 0.731, but the dichotomous range and extreme predictions weakened the predictive skill of this model compared to the thermodynamic approach.

The thermodynamic approach presented in this paper is a simple but effective means of estimating the injection height of smoke into the atmosphere. While more sophisticated modeling approaches can be used, the strength of this approach is in its simplicity – it can easily be integrated into current smoke forecasting systems such as BlueSky.

6. REFERENCES

- Anderson, K.R.; Englefield, P; Little, J.M.; Reuter, G. 2009. An approach to operational forest fire growth predictions for Canada. *Int. J. Wildland Fire* 18(8), 893–905.
- Anderson, K.R.; Pankratz, A; Mooney, C. 2011. A thermodynamic approach to estimating smoke plume heights. *In* 9th Symp. on Fire and Forest Meteorology, Oct 18-20, 2011. Palm Springs, CA. Am. Meteorol. Soc., Boston, MS. pp.
- Anderson, G.K.; Sandberg, D.V; Norheim, R.A. 2004. Fire Emission Production Simulator (FEPS) User's Guide Version 1.0. USDA For. Serv., Pacific Northwest Res.. Stn. 95 p.
- Briggs, G.A. 1972. Discussion: chimney plumes in neutral and stable surroundings. *Atmos. Envir.*, 6:507–510.
- Briggs, G.A. 1965. A plume rise model copared with observations. *J. Air Pollution Control Associ.* 15:433-438.
- Byram, G.M. 1959. Combustion of forest fuels. Pages 61-89 in K.P. Davis, ed, *Forest Fire: control and use*. McGraw-Hill Book Co., New York.
- Côté, J.; Gravel, S.; Méthot, A; Patoine, A.; Roch, M.; Staniforth, A. 1998 The operational CMC-MRB Global Environmental Multiscale (GEM) model: Part I - Design considerations and formulation. *Mon. Wea. Rev.* 126: 1373-1395.
- Forestry Canada Fire Danger Group. 1992. Development and structure of the Canadian Forest Fire Behavior Prediction System. Inf. Rep ST-X-3. Forestry Canada, Science and Sustainable Development Directorate, Ottawa, Ont., 63 pp.
- Goodrick, S.L; Achtemeier, G.L.; Larkin, N.K; Liu, Y.; Strand, T.M. 2013. Modelling smoke transport from wildland fires: a review. *International Journal of Wildland Fire* 2013, 22, 83–94
- Heilman, W.E; Liu, Y.; Urbanski, S.; Kovalev, V.; Mickler, R. 2014. Wildland fire emissions, carbon, and climate: Plume rise, atmospheric transport, and chemistry processes. *Forest Ecology and Management* 317 (2014) 70–79.
- Holzworth, C.G. 1967. Mixing depths, wind speeds and air pollution potential for selected locations in the United States. *J. Appl. Meteorol* 6, 1039-1044
- Larkin N.K.; O'Neill S.M.; Solomon R.; Raffuse S.; Strand T.; Sullivan D.; Krull C.; Rorig M.; Peterson J.; Ferguson S.A. 2009. The BlueSky smoke modeling framework. *Int. J. Wildland Fire* 18, 906–920.
- Larkin, N.K.; Strand T.M.; Drury S.A.; Raffuse S.M.; Solomon R.C.; O'Neill S.M.; Wheeler N.; Huang S-M.; Rorig M.; Hafner H.R. 2012. Phase 1 of the Smoke and Emissions Model Intercomparison Project (SEMIP): creation of SEMIP and evaluation of current models. Final Report to the Joint Fire Science Program, Project #08-1-6-10. *Chronicle* 65: 450-457.
- Raffuse, S.M.; Craig, K.J.; Larkin, N.K.; Strand, T.T.; Sullivan, D.C.; Wheeler, N.J.M.; Solomon, R. 2012. An evaluation of modeled plume injection height with satellite-derived observed plume height. *Atmosphere* 3, 103–123.
- Sofiev, M.; Ermakova, T.; Vankevich, R. 2006. Evaluation of the smoke-injection height from wild-land fires using remote-sensing data. *Atmos. Chem. Phys.*, 12, 1995–2006, 2012
- Van Wagner, C.E. 1987. Development and structure of the Canadian Forest Fire Weather Index System. *Can. For. Serv., Ottawa, Ont. For. Tech. Rep.* 35. 37 pp.

Table 2. Smoke plume observations

ID	Date (D-M-Y)	Time (MDT)	Observing Lookout Tower	Fire			Distance (km)	Adjusted equilibrium plume height (m)	Adjusted maximum plume height (m)	
				Number	Lat	Long				
1	20-7-10	1416	Keg	PWF104	57.59	-117.88	757	28.6	38	
2	20-7-10	1722	Keg	PWF126	57.42	-118.74	796	33.47	-312	
3	15-6-10	1715	Trout Mtn	SWF120	57.25	-113.57	774	71.62	2956	
6	14-5-10	1500	Whitefish	SWF116	56.53	-115.37	519	38.93	675	
7	19-6-10	1500	Whitefish	SWF137	56.55	-115.65	574	42.03	1400	4349
8	23-6-10	1557	Whitefish	SWF183	56.23	-114.97	579	31.59	510	
9	23-6-10	1724	Whitefish	PWF076	56.04	-116.04	654	38.41	867	1203
10	28-7-10	1601	Whitefish	SWF281	56.15	-115.45	686	3.63	113	368
11	18-6-10	945	Teepee Lk	SWF120	57.25	-113.57	774	93.84	1108	
12	18-6-10	954	Teepee Lk	SWF120	57.25	-113.57	774	93.84	1108	
13	18-6-10	1147	Teepee Lk	SWF120	57.25	-113.57	774	93.84	3976	
14	18-6-10	1550	Teepee Lk	SWF120	57.25	-113.57	774	93.84	7264	
15	20-6-10	1819	Teepee Lk	SWF118/120	57.26	-113.70	776	92.85	5550	
16	22-6-10	1401	Teepee Lk	SWF120	57.25	-113.57	774	93.84	1927	
17	22-6-10	1404	Teepee Lk	SWF120	57.25	-113.57	774	93.84	1927	
18	22-6-10	1414	Teepee Lk	SWF120	57.25	-113.57	774	93.84	2058	
19	22-6-10	1753	Teepee Lk	SWF120	57.25	-113.57	774	93.84	7264	
20	24-6-10	1446	Teepee Lk	SWF187	56.57	-114.41	728	21.61	374	
21	11-9-11	1600	Kirby Lk	Sask fire	55.75	-109.50	496	83.98	1847	
22	5-8-11	1935	Rainbow Lk	HWF112	58.75	-119.84	351	45.54	1208	
23	7-8-11	1658	Rainbow Lk	HWF116	59.39	-119.23	583	118.8	3199	
24	2-7-11	1333	Wadlin	SWF127	57.12	-115.16	477	75.63	2140	
25	2-7-11	1447	Wadlin	SWF127	57.12	-115.16	477	75.63	1480	
26	7-6-11	1434	Livock	MWF007	57.60	-111.30	301	164.3	2657	
27	7-6-11	1434	Livock	MWF007	57.60	-111.30	301	164.3	4760	
28	7-6-11	1914	Livock	MWF007	57.60	-111.30	301	164.3	8828	
31	8-7-12	1640	Hotchkiss	PWF060	57.15	-119.19	1011	24.44	1307	2595
32	8-7-12	1740	Hotchkiss	PWF060	57.15	-119.19	1011	24.4	878	2806
33	11-7-12	846	Hotchkiss	PWF068	57.15	-119.15	996	23.45	1472	2089
34	11-7-12	1041	Hotchkiss	PWF068	57.15	-119.15	996	23.45	1266	2709
35	11-7-12	1319	Hotchkiss	PWF068	57.15	-119.15	996	23.45	1266	3752
36	11-7-12	1555	Hotchkiss	PWF068	57.15	-119.15	996	23.45	1677	4597
37	11-7-12	1722	Hotchkiss	PWF068	57.15	-119.15	996	23.45	1677	7435
38	17-8-12	1822	Hotchkiss	PWF132	57.57	-119.97	950	66.1	3848	8505
39	26-5-12	1611	Hawk Hills	HWF070	57.92	-116.93	363	41.66	1594	2688
40	26-5-12	1700	Hawk Hills	HWF070	57.92	-116.93	363	41.66	1959	2688
41	26-5-12	1850	Hawk Hills	HWF070	57.92	-116.93	363	41.66	1959	2688
42	27-5-12	950	Hawk Hills	HWF070	57.92	-116.93	363	41.66	1230	1230
43	27-5-12	1900	Hawk Hills	HWF070	57.92	-116.93	363	41.66	2323	3053
44	4-7-12	1656	Hawk Hills	HWF070	57.92	-116.93	363	41.66	503	
45	20-5-12	1715	Pinto	GWFO32	54.78	-119.40	1044	18.74	41	
46	10-7-12	1500	Battle River	PWF068	57.15	-119.15	996	89.86	5021	
47	13-5-12	1729	Livock	SWF027	55.95	-113.91	554	79.31	866	2666
48	13-5-12	1745	Livock	SWF027	55.95	-113.91	554	79.31	1004	4747
49	11-5-12	1539	Saddle Hills	? (in BC)	56.07	-120.67	792	73.24	2514	3154
51	11-7-12	1612	Saddle Hills	PWF068	57.15	-119.15	996	173.4	5356	6871
52	11-7-12	1658	Saddle Hills	PWF068	57.15	-119.15	996	173.4	5356	6871
53	11-7-12	1941	Saddle Hills	PWF068	57.15	-119.15	996	173.4	6871	8387
54	14-9-12	1344	Saddle Hills	PWF166	56.61	-119.74	772	109.8	3057	4976
55	14-9-12	1705	Saddle Hills	PWF166	56.61	-119.74	772	109.8	3057	4976
56	18-9-12	1508	Saddle Hills	GWFO65	55.60	-119.52	898	12.47	517	1173
57	8-7-13	1752	Rainbow Lk	HWF097	58.47	-119.53	546	17.41	535	
59	10-5-13	1515	Pinto	GWFO07	55.03	-119.18	687	30.53	-636	
60	3-7-13	1910	Hotchkiss	HWF084	58.52	-117.80	422	132.2	1938	
61	4-7-13	1100	Hotchkiss	HWF084	58.52	-117.80	422	132.2	1938	
62	4-7-13	1200	Hotchkiss	HWF084	58.52	-117.80	422	132.2	1938	
64	21-6-13	1656	Livock	MWF041	56.23	-112.18	545	58.12	471	1384
65	24-5-13	835	May	LWF090	55.90	-112.46	571	37.48	-249	
67	24-5-13	957	May	LWF090	55.90	-112.46	571	37.48	405	1715
68	24-5-13	1041	May	LWF090	55.90	-112.46	571	37.48	1715	4349
69	24-5-13	1100	May	LWF090	55.90	-112.46	571	37.48	405	3028
70	24-5-13	1201	May	LWF090	55.90	-112.46	571	37.48	78	1715
71	24-5-13	1402	May	LWF090	55.90	-112.46	571	37.48	405	4681
72	24-5-13	1515	May	LWF090	55.90	-112.46	571	37.48	732	1715
73	24-5-13	1705	May	LWF090	55.90	-112.46	571	37.48	78	3688
74	31-5-13	1424	May	LWF101	55.75	-112.71	551	28.1	-114	868
75	31-5-13	1443	May	LWF101	55.75	-112.71	551	28.1	868	1359
76	31-5-13	1537	May	LWF101	55.75	-112.71	551	28.1	-114	868
77	19-5-13	1400	Ponton	HWF028	59.63	-117.10	311	92.31	1311	1311
78	19-5-13	1459	Ponton	HWF028	59.63	-117.10	311	92.31	1311	2117
79	25-5-13	1421	Ponton	HWF037	58.45	-116.63	298	58.89	1442	2471
80	25-5-13	1443	Ponton	HWF037	58.45	-116.63	298	58.89	928	1956
81	25-5-13	1548	Ponton	HWF037	58.45	-116.63	298	58.89	1442	2986
82	25-5-13	1640	Ponton	HWF037	58.45	-116.63	298	58.89	928	2986
83	25-5-13	1740	Ponton	HWF037	58.45	-116.63	298	58.89	-100	
84	27-5-13	1646	Ponton	HWF039	58.94	-115.55	909	38.39	831	2509
85	27-5-13	1711	Ponton	HWF039	58.94	-115.55	909	38.39	831	1501

Table 3. Predicted plume heights

ID	Lapse rate (°C)*					Predicted Plume Height (m) using:					Briggs Model (m)	Mixing Layer (m)	
	<i>T_s-T₈₅₀</i>	<i>T_s-T₇₀₀</i>	<i>T_s-T₅₀₀</i>	<i>T₈₅₀-T₇₀₀</i>	<i>T₈₅₀-T₅₀₀</i>	<i>T_s-T₈₅₀</i>	<i>T_s-T₇₀₀</i>	<i>T_s-T₅₀₀</i>	<i>T₈₅₀-T₇₀₀</i>	<i>T₈₅₀-T₅₀₀</i>			
1	-10.20	-9.62	-7.86	-9.34	-7.43		1230	1027	1230	986	1	3305	
2	-10.03	-8.22	-7.28	-7.54	-6.89		1151	1047	1070	1016	1	3068	
3	-10.16	-9.82	-8.30	-9.65	-7.95			3171	3650	3022	762	3591	
6	-10.29	-9.86	-8.04	-9.63	-7.58			2596	3101	2461	312	4164	
7	-10.10	-9.81	-8.12	-9.69	-7.78			3034	3563	2917	1319		
8	-9.47	-8.64	-7.39	-8.21	-6.98	2307	2138	1839	2003	1781	20	2954	
9	-9.50	-8.67	-7.37	-8.25	-6.95	2401	2238	1912	2095	1851	34	2957	
10	-10.03	-8.13	-7.58	-7.17	-7.11			623	588	567	565	0	2638
11	-8.71	-9.24	-8.04	-9.47	-7.93	5654	6086	5051	6086	4979	2274	4379	
12	-8.71	-9.24	-8.04	-9.47	-7.93	5862	6302	5247	6302	5174	2272	4379	
13	-10.50	-9.94	-8.35	-9.70	-8.00			6776	7773	6445	3959	4749	
14	-10.19	-9.91	-8.69	-9.79	-8.45			10384	11247	9891	8590	5129	
15	-10.99	-9.84	-8.53	-9.42	-8.20			7242	8025	6879	3448		
16	-10.11	-7.67	-6.96	-6.54	-6.41		6704	6290	6104	6051	5688	2984	
17	-10.11	-7.67	-6.96	-6.54	-6.41		6449	6036	5851	5797	5904	2984	
18	-10.11	-7.67	-6.96	-6.54	-6.41		5998	5587	5404	5351	6588	2984	
19	-9.88	-7.85	-7.30	-6.92	-6.85		8012	7555	7303	7267	8067	2991	
20	-9.65	-7.75	-6.88	-6.87	-6.40	2367	1949	1812	1812	1757	9	2956	
21	-7.99	-5.80	-6.21	-4.69	-5.88	2495	2117	2165	2013	2125	26	2118	
22	-9.34	-7.75	-7.06	-6.84	-6.56	1990	1634	1537	1512	1484	90	2018	
23	-9.86	-7.04	-6.53	-5.37	-5.78		3487	3355	3134	3204	1039	2004	
24	-10.37	-8.43	-7.37	-7.38	-6.75		2188	1940	1941	1850	122	2925	
25	-10.37	-8.43	-7.37	-7.38	-6.75		1655	1473	1473	1407	0	3440	
26	-10.09	-8.25	-7.30	-7.20	-6.70		10190	9064	8978	8604	11970	2885	
27	-10.09	-8.25	-7.30	-7.20	-6.70		9718	8603	8518	8148	12541	3442	
28	-9.52	-8.02	-7.14	-7.15	-6.62	14435	11672	10522	10530	10052	14451	2239	
31	-9.82	-8.85	-7.47	-8.46	-7.11		3095	2563	2880	2488	913	3194	
32	-9.82	-8.85	-7.47	-8.46	-7.11		4163	3443	3872	3342	1395	3194	
33	-2.56	-5.46	-6.98	-6.51	-7.58	1814	2011	2195	2128	2307	83	794	
34	-2.56	-5.46	-6.98	-6.51	-7.58	2111	2358	2590	2505	2730	208	794	
35	-10.47	-7.03	-7.34	-5.77	-6.91		4339	4457	3994	4299	1263	2129	
36	-10.25	-8.22	-7.56	-7.46	-7.18		6438	5920	5861	5702	2825	3139	
37	-9.98	-8.96	-7.44	-8.58	-7.08		8796	6863	8047	6638	3631	3518	
38	-9.74	-8.07	-6.87	-7.41	-6.44	9458	7861	6931	7277	6711	9027	2491	
39	-10.07	-9.40	-8.06	-8.95	-7.56		2687	2273	2654	2151	40	3586	
40	-9.87	-9.53	-8.18	-9.30	-7.76		2986	2559	2986	2431	52	3595	
41	-9.87	-9.53	-8.18	-9.30	-7.76		3772	3255	3772	3101	41	3595	
42	-4.36	-7.15	-6.74	-8.99	-7.33	1477	1713	1663	2189	1738	4	993	
43	-9.91	-9.37	-8.09	-9.02	-7.64		4805	4046	4805	3836	190	3610	
44	-9.77	-9.53	-7.62	-9.38	-7.10	6492	6492	5111	6492	4859	439	3233	
45	-9.98	-9.83	-7.77	-9.77	-7.46			634	768	616	0	3833	
46	-10.34	-8.61	-7.22	-7.97	-6.79							2802	
47	-10.00	-9.90	-8.12	-9.84	-7.74			1944		1855	112	3167	
48	-10.00	-9.90	-8.12	-9.84	-7.74			2289		2184	218	3167	
49	-10.41	-7.99	-6.86	-6.79	-6.19		3653	3271	3253	3123	96	3072	
51	-10.25	-8.22	-7.56	-7.46	-7.18		6506	5974	5914	5750	3051	3139	
52	-9.98	-8.96	-7.44	-8.58	-7.08		8084	6245	7371	6032	3587	3518	
53	-9.14	-9.53	-7.22	-9.67	-6.95	10046	10046	7538	10046	7361	4047	3142	
54	-10.39	-9.43	-7.44	-9.08	-7.02		3820	3019	3820	2916	64	2687	
55	-9.90	-9.29	-7.05	-9.05	-6.64		5238	3804	5238	3670	191	2693	
56	-10.22	-7.48	-5.99	-6.34	-5.33		2227	1974	2021	1899	83	2414	
57	-9.76	-9.33	-8.12	-9.08	-7.75	1740	1740	1490	1740	1429	24	5247	
59	-10.36	-7.16	-6.86	-5.80	-6.30		1175	1147	1069	1103	6	2415	
60	-9.73	-9.02	-7.16	-8.75	-6.80	3435	3435	2639	3238	2565	286	2439	
61	-8.52	-7.44	-6.75	-7.03	-6.49	3346	2932	2773	2832	2725	112	3108	
62	-9.13	-7.79	-6.91	-7.29	-6.59	3973	3246	2996	3089	2927	176	3482	
64	-9.88	-9.14	-7.99	-8.72	-7.58		2550	2117	2380	2020	311	3586	
65	-6.21	-6.01	-6.09	-5.91	-6.06	496	491	493	488	492	0	1601	
67	-8.69	-6.57	-6.34	-5.57	-5.92		695	667	632	641	0	1855	
68	-10.48	-7.23	-6.63	-5.67	-5.94		729	699	662	671	0	2128	
69	-10.48	-7.23	-6.63	-5.67	-5.94		969	894	875	858	0	2128	
70	-10.48	-7.75	-6.78	-6.45	-6.11		1885	1617	1690	1551	0	2439	
71	-10.36	-8.39	-6.93	-7.46	-6.32		2351	1981	2109	1902	17	2771	
72	-10.28	-8.54	-7.03	-7.72	-6.45		3364	2592	3166	2500	29	2774	
73	-9.99	-9.13	-7.03	-8.73	-6.51	2138	1939	1663	1811	1611	38	2775	
74	-9.53	-8.52	-7.08	-8.01	-6.62		2197	1715	1827	1669	5	2809	
75	-9.20	-8.29	-7.12	-7.84	-6.73	1873	1806	1714	1777	1692	5	2811	
76	-7.84	-7.46	-6.79	-7.27	-6.59		3391	2761	3171	2655	12	2473	
77	-10.12	-9.15	-7.74	-8.71	-7.33		5370	4469	5370	4286	507	3463	
78	-10.23	-9.77	-7.95	-9.56	-7.56		2242	1756	2242	1687	1557	3848	
79	-10.17	-9.49	-7.37	-9.17	-6.88		2624	2072	2521	1995	34	3501	
80	-10.12	-9.24	-7.36	-8.83	-6.87		3229	2570	3229	2470	40	3889	
81	-10.11	-9.59	-7.55	-9.35	-7.10		3566	2851	3566	2738	64	3506	
82	-10.06	-9.58	-7.68	-9.36	-7.27		4013	3208	4013	3083	91	3508	
83	-9.99	-9.59	-7.69	-9.41	-7.29	3176	2728	2494	2588	2437	147	3509	
84	-9.48	-8.20	-7.40	-7.77	-7.13	3906	3369	3089	3201	3021	807	2093	
85	-9.48	-8.20	-7.40	-7.77	-7.13		1230	1027	1230	986	1131	2093	

Lapse rates shown in italics are superadiabatic. Lapse rates exceeding -9.00 °C/km were set to -9.00 °C/km for plume rise calculations.

Table 4. Summary of correlation coefficients between predicted and observed plume heights.

Lapse rate used	All observations	n	Daily average observation	n	Observation closest to 17:00 LST	n
$T_{Sfc}-T_{850}$	0.755	22	0.459	12	0.812	12
$T_{Sfc}-T_{700}$	0.550	61	0.617	30	0.627	29
$T_{Sfc}-T_{500}$	0.636	70	0.669	37	0.775	36
$T_{850}-T_{700}$	0.617	68	0.633	36	0.687	35
$T_{850}-T_{500}$	0.635	70	0.669	37	0.773	36
Average*	0.617		0.652		0.730	
Brigg's	0.504	70	0.481	37	0.731	36
Mixing Layer	0.011	70	0.0005	37	0.0004	36

* Average values exclude predictions based on the surface to 850 hpa lapse rate